THE BELL SYSTEM TECHNICAL JOURNAL
Vol. 54, No. 6, July–August 1975
Printed in U.S.A.

A Method for Calculating Rain Attenuation Distributions on Microwave Paths

By S. H. LIN

(Manuscript received January 9, 1975)

An engineering method is proposed for calculating rain attenuation distributions for frequencies greater than 10 GHz and for paths of arbitrary length. The technique is based upon the observed approximate lognormality of rain attenuation and rain rate statistics within the range of interest; it reflects local meteorology through incorporation of the observed point rain rate distribution. Some important parameters in the resulting formulas are determined empirically from experimental data. Sample calculated results agree well with available experimental data from Georgia, New Jersey, and Massachusetts. This new technique may prove useful for engineering radio paths at frequencies above 10 GHz. Sample calculations of expected outage probability are given for 11- and 18-GHz radio links at Atlanta, Georgia, as a function of repeater spacing and transmission polarization.

I. INTRODUCTION

An important problem in designing radio relay systems at frequencies above 10 GHz is the radio outage caused by rain attenuation. Determination of the appropriate radio repeater spacings for economic and reliable operation requires a knowledge of the probability distribution of rain attenuation as a function of repeater spacing at various geographic locations. Most available data on rain rate statistics are measured by a single rain gauge at a given geographic location. A procedure for calculating a rain attenuation distribution from a point rain rate distribution is, therefore, needed.

The results of rain gauge network measurements[1–5] indicate, however, that the measured short-term distributions of point rain rate vary significantly from gauge to gauge. For example, at Holmdel, New Jersey, there was considerable variation[1] among the measured point rain rate distributions obtained from 96 rain gauges located in a grid with 1.3-km spacing over a 6-month period. Among these 96 distributions, the incidence of 100-mm/h rains is higher by a factor of

5 for the upper quartile gauges than for the lowest quartile (see Fig. 32, Ref. 1). Data from a rain gauge network in England[5] indicate that even with a 4-year time base and averaging over observations by four gauges with 1-km gauge spacing, the four-gauge-average rain rate incidence can differ by a factor of 3 for rain rates above 80 mm/h, depending on which four gauges are chosen for averaging. This means that, on a short-term basis, the relationship between the path rain attenuation distribution and the rain rate distribution measured by a single rain gauge is *not unique*. The prediction of a path rain attenuation distribution from a point rain rate distribution is, therefore, meaningful only if the time base is sufficiently long to yield stable, representative statistics. Accordingly, knowledge of the long-term statistical behavior of point rain rate and path rain attenuation is essential for radio path design.

The available experimental rain data (Appendix B, Figs. 10 to 13, and Ref. 6) indicate that the long-term distributions of point rain rate R and rain attenuation α are approximately lognormal within the range of interest to designers of radio paths using frequencies above 10 GHz. This paper describes a method for calculating rain attenuation distributions based upon this lognormal hypothesis.

A lognormal distribution is uniquely determined by three parameters (see Section 2.1). A set of equations are derived to relate the lognormal parameters of attenuation α to those of point rain rate R. Thus, given a long-term, representative distribution of point rain rate at a given geographic location, the rain attenuation distribution for any path length of interest can be calculated. The method is outlined as follows.

The available theory[7–13] for converting rain rate R into rain attenuation gradient β in dB/km is appropriate to spatially uniform rain rates, whereas actual rainfalls are usually not uniform over an entire radio path. To apply the uniform rain theory, the radio path volume is divided into small incremental volumes ΔV, in which the rain rate is approximately uniform. The rain rate R in each small volume ΔV is associated with a corresponding attenuation gradient β by the uniform rain theory. The total path attenuation α is then the integral of β over the path volume.

If the spatial distribution of the attenuation gradient β were uniform, the path attenuation at a given probability level would increase linearly with path length. On the other hand, if the spatial distribution of βs were not uniform and the time fluctuations of the βs were statistically independent, the incremental attenuation contributed by each ΔV would sum on an rms basis. Intuitively, we feel that the attenuation gradients at two different positions are partially corre-

lated, with a correlation coefficient that is a decreasing function of the spacing between the two positions. This behavior is described by introducing a spatial correlation function for β. This spatial correlation function is used in the calculation of lognormal parameters of path attenuation α from those of attenuation gradient β.

In this formulation, the appropriate incremental sampling volume ΔV is of the order of 1 m^3 and the corresponding appropriate rain gauge integration time about 2 s, requiring, therefore, 2-s point rain rate distributions (see Section 2.3).

Tables II and III and Figs. 5 to 8, discussed in Section IV, present comparisons of calculated and measured attenuation distributions. The satisfactory correspondence appears to validate the method of calculation. Section V and Fig. 9 present the calculated results for the outage probabilities of 11- and 18-GHz radio links in Georgia. Section VI discusses some qualifications to the methodology.

Supporting material and mathematical derivations are given in Appendices A to D. Appendix E lists symbols and their definitions.

II. BASIC DEFINITIONS AND FORMULATION

2.1 Lognormal distributions of attenuation and rain rate

The equations approximating the rain attenuation distribution and point rain rate distribution are:

$$P[\alpha(L) \geqq A] \simeq P_0(L) \cdot \tfrac{1}{2}\mathrm{erfc}\left[\frac{\ln A - \ln \alpha_m}{\sqrt{2}S_\alpha}\right] \tag{1}$$

and

$$P(R \geqq r) \simeq P_0(0) \cdot \tfrac{1}{2}\mathrm{erfc}\left[\frac{\ln r - \ln R_m}{\sqrt{2}S_R}\right], \tag{2}$$

where erfc ($\sim$) denotes the complementary error function, ln ($\sim$) denotes natural logarithm, S_α and S_R are the standard deviations of ln α and ln R, respectively, *during the raining time*, α_m and R_m are the median values of α and R, respectively, during the raining time, $P_0(L)$ is the probability that rain will fall on the radio path of length L, and $P_0(0)$ is the probability that rain will fall at the point where the rain rate R is measured. The definition and the determination of raining time, and hence $P_0(L)$ and $P_0(0)$, are discussed in Section 2.5. The measured distribution of point rain rate is a function of rain gauge integration time T.[14-20] The appropriate integration time is about 2 s in our formulation as discussed in Section 2.3.

2.2 Radio path definition

C. L. Ruthroff[21] has defined a "radio path," giving a physical as well as mathematical representation in the spatial volume significant

to propagation considerations (Fig. 1). In essence, the "radio path" corresponds to the first Fresnel zone, a prolate ellipsoid of revolution terminated at the ends by the transmitting and receiving antennas.

Since the first Fresnel zone is circularly symmetric with respect to the path axis connecting the transmitting and receiving antennas, we adopt a cylindrical coordinate system (Fig. 1) coaxial with the path axis (z-axis) in the formulation.

The radius $h(z)$ and the circular cross section $Q(z)$ (see Fig. 1) of the radio beam at a distance z from the transmitter are

$$h(z) = \left[\frac{\lambda \cdot z(L - z)}{L} \right]^{\frac{1}{2}} \tag{3}$$

and

$$Q(z) = \pi h^2(z), \tag{4}$$

where λ is the radio wavelength and L is the distance between transmitter and receiver. For example, at 18 GHz on a 5-km path, the average beam radius, the average beam cross section, and the radio path volume are about 3 m, 30 m^2, and 150,000 m^3, respectively.

2.3 Path integral formulation for rain attenuation

The spatial distribution of actual rainfall is usually nonuniform. The rain density, the point rain rate R, and the corresponding (point) rain attenuation gradient β are all functions of position (ρ, ϕ, z) and of time (t). The total rain attenuation α in dB incurred on a radio path of length L (Fig. 1) is calculated by integrating the incremental attenuation $d\alpha$ along the path

$$\alpha(t) = \int_0^L \frac{d\alpha}{dz}\, dz = \int_0^L \beta_q(z, t) dz \tag{5}$$

$$= \int_0^L \frac{1}{Q(z)} \int_{\phi=0}^{2\pi} \int_{\rho=0}^{h(z)} \beta(\rho, \phi, z, t) \rho d\rho d\phi dz, \tag{6}$$

where

$$\beta_q(z, t) = \frac{1}{Q(z)} \int_{\phi=0}^{2\pi} \int_{\rho=0}^{h(z)} \beta(\rho, \phi, z, t) \rho d\rho d\phi \tag{7}$$

is the average value of $\beta(\rho, \phi, z, t)$ over the radio beam cross section $Q(z)$ at a distance z from the transmitter, and

$$d\alpha(z, t) = \beta_q(z, t) dz \tag{8}$$

is the incremental attenuation experienced in the incremental segment dz at a distance z from the transmitter.

To shorten the notations in the following equations, we use the vector $\mathbf{s}$ to denote the position (ρ, ϕ, z) and dv to denote $\rho d\rho d\phi dz$ in the volume integration.

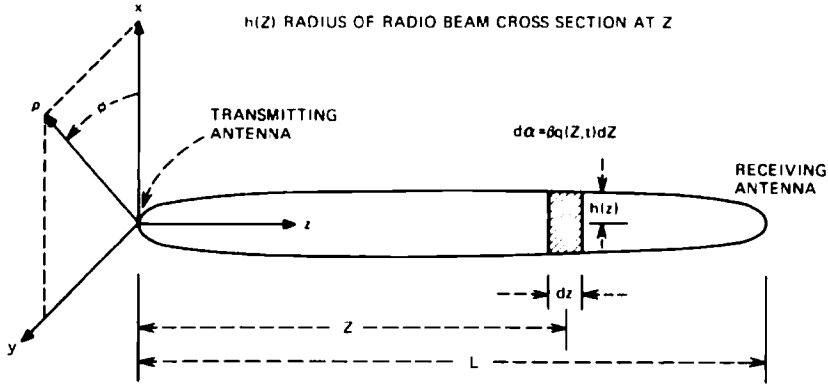

Fig. 1—Configuration of a radio path.

The rain density and the rain attenuation gradient β in dB/km are only meaningful with respect to a sampling volume ΔV large enough to contain sufficient raindrops to yield stable volume average quantities. The results of measurements of rain density and rain rate by a photographic method[22] indicate that the typical rain density at 1-mm/h rain rate varies from 50 to 100 raindrops per m^3, depending on geographic location. This means, on the average, a 0.1-m^3 volume contains only 2 raindrops at 0.25-mm/h rain rate. Such a small sampling volume will not measure the rain rate in the conventional sense, but rather will "see" individual raindrops. Thus, for a meaningful measurement of rain rate below 1 mm/h, the sampling volume should be at least 1 m^3.

On the other hand, the available theoretical results[7-13] relating β and R assume that the rain density is uniform within the volume of interest. To use the available functional relationship $\beta(R)$ to convert the statistics of R into that of β, the sampling volume ΔV must be sufficiently small so that the rain density (and the rain rate) is approximately uniform within ΔV. The observations by a capacitor flow rain gauge[23,24] and by a raindrop photographic method[25] indicate that heavy rain has fine scale structure on the order of 1 m. This means ΔV should not be much larger than 1 m^3.

These two constraints indicate that the sampling volume should be on the order of 1 m^3. We have chosen*

$$\Delta V \approx 1 \text{ m}^3 \tag{9}$$

in our formulation.

* A choice of ΔV somewhat different from 1 m^3 is also possible. Since the spatial correlation coefficient of β depends on the sampling volume, the use of a slightly different ΔV would result in a slightly different characteristic distance G, defined in eq. (35) and determined in Section 4.1. For example, a larger sampling volume, with more smoothing effect, will result in a larger characteristic distance G for β.

Therefore, in this paper, $\beta(\mathbf{s}, t)$ is defined as the rain attenuation gradient at time t, owing to rain in a 1-m³ sampling volume, ΔV, centered at $\mathbf{s}$, and $\beta_q(z, t)$ is the average value of $\beta(\mathbf{s}, t)$ over the path cross section $Q(z)$.

If A_g is the area of the collecting aperture of a rain gauge and V_R the average descent velocity of rainfall, then the appropriate rain gauge integration time $T_{\Delta V}$ to measure rain rate in a 1-m³ sampling volume ΔV is

$$T_{\Delta V} \simeq \frac{\Delta V}{A_g \cdot V_R}. \tag{10}$$

For example, if $A_g = 0.073$ m² (i.e., 12-in. diameter), then $T_{\Delta V}$ is about 2 s, assuming $V_R \cong 7$ m/s. In the measurements of raindrop size distributions, Laws and Parsons[26] have also used an integration time in the order of seconds during heavy rain. The Laws-and-Parsons raindrop size distribution is the basis of most uniform rain theories for converting R into β. We therefore define $R(\mathbf{s}, t)$ as the point rain rate measured by a rain gauge with integration time $T_{\Delta V}$, located at $\mathbf{s}$. The shape of the 1-m³ sampling volume defined by the rain gauge is cylindrical and is considerably different from that of the incremental ΔV. We assume that the long-term distributions of rain rates for these two different shapes of 1-m³ sampling volume are approximately the same.

Based upon these definitions, we postulate that the long-term probability distribution of $R(\mathbf{s}, t)$ can be converted into the long-term probability distribution of $\beta(\mathbf{s}, t)$ by a relationship discussed in the next section.

The integration times of most available point rain rate data are longer than the $T_{\Delta V}$ ($\cong$2 s) required by this formulation. The dependence of point rain rate distribution on the rain gauge integration time in the range

$$1.5 \text{ s} \leqq T \leqq 120 \text{ s} \tag{11}$$

has been determined by Bodtmann and Ruthroff[15] for a 2-year (1971-1972) measurement at Holmdel, New Jersey. By using this experimental result and interpolation, we convert the available point rain rate distribution with T in the range (11) into a 2-s point rain rate distribution.*

2.4 Average relationship between rain rate and rain attenuation gradient

The instantaneous relationship obtaining between the point rain rate $R(\mathbf{s}, t)$ and the corresponding rain attenuation gradient $\beta(\mathbf{s}, t)$

* This relationship has not yet been demonstrated to be geographically independent.

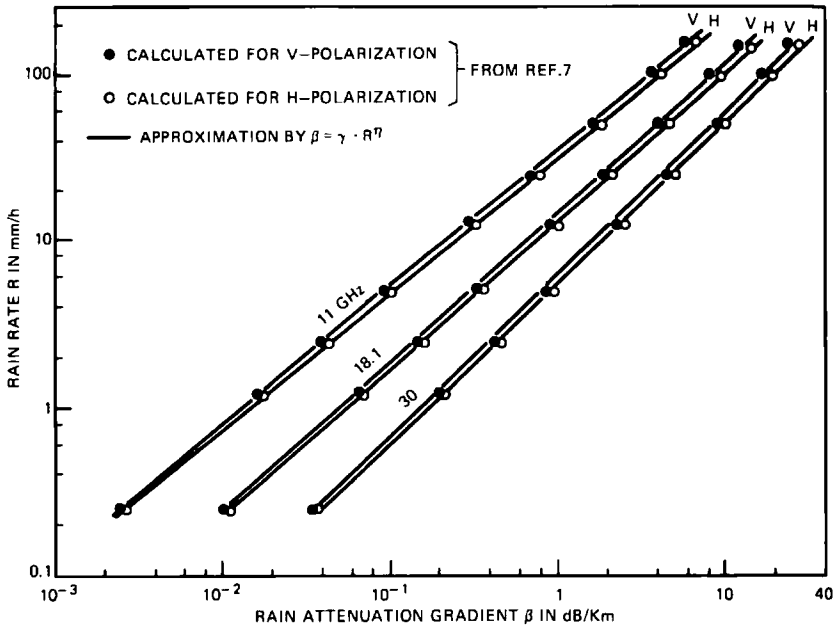

Fig. 2—Theoretical relationship between rain rate and rain attenuation gradient.

depends upon the particular distribution of raindrop sizes, shapes, and orientations, the speed and local direction of the wind, and the rain temperature. The average relationship, assuming uniform rain density, spherical raindrops, and Laws-and-Parsons drop-size distribution, has been calculated by Ryde and Ryde,[11–13] Medhurst,[9] and Setzer.[10] Recently, Morrison, Cross, and Chu,[7,27] and Oguchi[8] have refined these calculations by including the effects of nonspherical raindrops. Figure 2 shows this theoretical relationship* for transmission frequencies of 11, 18, and 30 GHz.

Many authors have pointed out that this average relationship between the rain rate R and rain attenuation gradient β can be approximately described by

$$\beta = \gamma(\lambda) \cdot R^{\eta(\lambda)}, \tag{12}$$

where $\gamma(\lambda)$ and $\eta(\lambda)$ depend upon the radio wavelength λ and the polarization of the radio signal. Table I lists the estimated $\gamma(\lambda)$ and $\eta(\lambda)$ for 11, 18, 30, and 60 GHz.

* In Fig. 2, the average of the absolute value of raindrop canting angle is assumed to be 25 degrees. This angle has been found representative by Chu (Refs. 28 and 29) in comparisons of calculated results with experimental observations (Refs. 30 and 31) of the differential rain attenuation experienced by horizontally and vertically polarized signals on the same radio path.

Table I — Parameters relating rain rate R and rain attenuation gradient β

$\beta = \gamma \cdot R^{\eta}$ β in dB/km R in mm/hour

Frequency (GHz)	γ		η	
	V-Pol	H-Pol	V-Pol	H-Pol
11	0.013	0.015	1.22	1.23
18.1	0.05	0.054	1.11	1.14
30	0.15	0.17	1.04	1.04
60*	0.7*	0.7*	0.814*	0.814*

* The 60-GHz parameters are estimated from results in Ref. 10 in which only spherical raindrops are considered.

Taking logarithms of both sides of eq. (12) yields

$$\ln \beta = \ln \gamma + \eta \cdot \ln R. \tag{13}$$

From this equation, if the distribution of point rain rate R is approximately lognormal in the range of interest, then the distribution of attenuation gradient β will also be approximately lognormal (see Appendix B). The distribution of β can therefore be written as:

$$P(\beta \geqq B) \simeq P_0(0) \cdot \tfrac{1}{2}\mathrm{erfc}\left[\frac{\ln B - \ln \beta_m}{\sqrt{2} \cdot S_\beta}\right], \tag{14}$$

where β_m is the median value of β during the raining time and S_β is the standard deviation of $\ln \beta$ during the raining time. Furthermore, eqs. (12) and (13) imply the relationships

$$S_\beta = \eta \cdot S_R \tag{15}$$

and

$$\beta_m = \gamma \cdot R_m^{\eta}. \tag{16}$$

Equations (15) and (16) allow us to convert the lognormal distribution (2) of R into the lognormal distribution (14) of β, and vice versa.

2.5 Rainfall probability $P_0(0)$ and raining time

In principle, the probability of raining, $P_0(0)$, is obtained as the limit

$$\lim_{\epsilon \to 0^+} P(R \geqq \epsilon) \equiv P_0(0). \tag{17}$$

An instant t is considered to be raining time if the condition

$$\lim_{\epsilon \to 0^+} R(t) > \epsilon \tag{18}$$

is satisfied. The lower cutoff threshold in most presently available rain

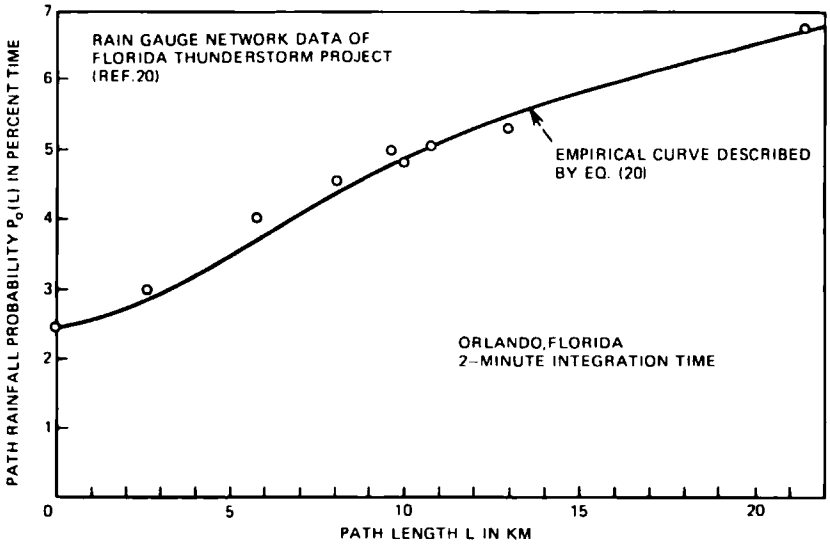

Fig. 3—Rain-gauge network data on path length dependence of rainfall probability $P_0(L)$.

rate data is about 0.25 mm/h. Therefore, in practice, we approximate 0^+ in definitions (17) and (18) by 0.25 mm/h. The rationale for this approximation is twofold.

(*i*) Rain rates below 0.25 mm/h have practically no significant effects on radio communication links at frequencies below 60 GHz.

(*ii*) Rain rates below 0.25 mm/h cannot be measured accurately by most existing rain gauges with standard recording strip charts.

At the present time, the probability $P(R \geqq 0.25 \text{ mm/h} \mid T = 1 \text{ min})$ is available at only a few locations.[14,18,20] For most locations, we can obtain $P(R \geqq 0.25 \text{ mm/h})$ with 1-h integration time from the Weather Bureau hourly precipitation data.[32] The experimental results on the effect of rain gauge integration time T on $P_0(0)$ in Florida[14,20] and Japan[18] indicate that

$$P(R \geqq 0.25 \text{ mm/h} \mid T \leqq 1 \text{ min}) \simeq 0.5 \cdot P(R \geqq 0.25 \text{ mm/h} \mid T = 1 \text{ h}). \quad (19)$$

Therefore, we use Weather Bureau data and approximation (19) to estimate $P_0(0)$ at several locations of interest where direct measurement of $P_0(0)$ with 1-min integration is not available.

Intuitively, we expect the probability $P_0(L)$ of rainfall on a radio path of length L to increase with L, since a longer path has a higher chance of intercepting rain of limited extent. From the rain gauge network data (Fig. 3) of the Florida Thunderstorm Project,[14] we obtain the empirical formula

$$P_0(L) \cong 1 - \frac{1 - P_0(0)}{\left[1 + \frac{L^2}{21.5}\right]^{0.014}}, \tag{20}$$

where L is in units of kilometers and

$$P_0(0) = \lim_{L \to 0} P_0(L) \tag{21}$$

is the point rain probability that depends on geographic location. A theoretical consideration leading to the empirical form (20) is discussed in Appendix C.

III. OUTLINE FOR CALCULATING RAIN ATTENUATION DISTRIBUTION

3.1 Path length dependence of median attenuation α_m and standard deviation S_α

From the lognormal approximations (1) and (14), it can be shown[23] that:

$$S_\alpha^2 = \ln\left\{1 + \frac{\sigma_\alpha^2}{\bar{\alpha}^2}\right\} \tag{22}$$

$$S_\beta^2 = \ln\left\{1 + \frac{\sigma_\beta^2}{\bar{\beta}^2}\right\} \tag{23}$$

$$\alpha_m = \bar{\alpha} \cdot \exp\left[\frac{-S_\alpha^2}{2}\right] \tag{24}$$

$$\beta_m = \bar{\beta} \cdot \exp\left[\frac{-S_\beta^2}{2}\right], \tag{25}$$

where

$$\bar{\alpha} = E_L\{\alpha(t)\} \tag{26}$$

$$\bar{\beta} = E_0\{\beta(t)\} \tag{27}$$

$$\sigma_\alpha^2 = E_L\{\alpha^2(t)\} - \bar{\alpha}^2 \tag{28}$$

and

$$\sigma_\beta^2 = E_0\{\beta^2(t)\} - \bar{\beta}^2. \tag{29}$$

$E_L\{\sim\}$ denotes a statistical (time) average under the condition that rain is falling on the radio path of length L, $E_0\{\sim\}$ denotes statistical (time) average under the condition that rain is falling at the location

of interest. In eqs. (27) and (29), we assume that the long-term, large-sample, conditional statistical average $\bar{\beta}$ and variance σ_β^2 are independent of position s in or near the radio path of interest. Therefore, we omit the position s argument in these equations.

By using eqs. (6), (22), (23), (24), and (25), we can derive formulas for the dependence of $S_\alpha(L)$ and $\alpha_m(L)$ on the radio path length L. The lengthy derivations are given in Appendix A. The results are

$$S_\alpha^2(L) = \ln P_0(L) \left\{1 + H(L) \left[\frac{\exp(S_\beta^2)}{P_0(0)} - 1 \right] \right\} \tag{30}$$

and

$$\alpha_m(L) = \beta_m \cdot L \cdot \frac{P_0(0)}{P_0(L)} \cdot \exp\left[\frac{S_\beta^2 - S_\alpha^2}{2} \right], \tag{31}$$

where

$$H(L) = \frac{1}{L^2} \int_0^L \int_0^L \frac{1}{Q(z)} \int_{Q(z)} \int \frac{1}{Q(z')} \int_{Q(z')} \int \psi_u(\mathbf{s}, \mathbf{s}') dv dv', \tag{32}$$

$$\psi_u(\mathbf{s}, \mathbf{s}') = \frac{1}{\sigma_{\beta u}^2} \{E_u[\beta(\mathbf{s}, t) \cdot \beta(\mathbf{s}', t)] - \bar{\beta}_u^2\} \tag{33}$$

is the spatial correlation coefficient[34,35] between $\beta(\mathbf{s}, t)$ and $\beta(\mathbf{s}', t)$, and

$$C_\beta(\mathbf{s}, \mathbf{s}') = \sigma_{\beta u}^2 \cdot \psi_u(\mathbf{s}, \mathbf{s}') \tag{34}$$

is the spatial covariance function[34,35] of $\beta(\mathbf{s}, t)$ and $\beta(\mathbf{s}', t)$, $E_u\{\sim\}$ denotes the unconditional statistical (time) average including both raining time and nonraining time, $\bar{\beta}_u$ and $\sigma_{\beta u}^2$ are the unconditional statistical mean and variance, respectively, of β as defined by eqs. (48) and (49) in Appendix A.

In eq. (32), the integration volume is the entire radio path (Fig. 1) and is a function of both path length L and wavelength λ. However, the spatial correlation coefficient ψ_u of (point) rain attenuation gradient β defined in eq. (33) is not a function of radio path length L.

If the random fluctuations of the βs were "coherent" along the entire radio path, then ψ_u, $H(L)$ and $P_0(L)/P_0(0)$ would be identically unity. Under such conditions, S_α would be identical to S_β and $\alpha_m(L)$ would be equal to $\beta_m \cdot L$ as expected. The complexity of path length dependencies of S_α and α_m in eqs. (30) to (34) is caused by the partially correlated, random fluctuations of βs at various points in the radio path.

We postulate ψ_u to have the functional dependence on distance

$$\psi_u = \frac{G(\lambda, \Delta V)}{[G^2(\lambda, \Delta V) + d^2]^{\frac{1}{2}}} \tag{35}$$

within the range of interest, where

$$d = |\mathbf{s} - \mathbf{s}'|$$

is the distance between the two observation points (s) and (s'), and $G(\lambda, \Delta V)$ is a characteristic distance at which $\psi_u = 1/\sqrt{2}$. The dependence of β on wavelength λ (Fig. 2) and sampling volume ΔV (Section 2.3) indicates that the characteristic distance G may also be a function of λ and ΔV. However, in Table I, the exponents η are all very close to unity for frequencies ranging from 11 to 60 GHz. This means β is approximately *linearly* proportional to R in this frequency range. Therefore, the characteristic distance G of β is approximately equal to that of point rain rate R and will not be very sensitive to frequency in the range from 11 to 60 GHz.

Substituting (35) into (32) and carrying out integrations over ρ' and ϕ' yield

$$H(L) = \frac{4\pi G}{L^2} \cdot \int_0^{\pi} d\theta \int_0^{L} \frac{dz}{Q(z)} \int_0^{h(z)} \rho d\rho \int_0^{L} \frac{F dz'}{Q(z')}, \tag{36}$$

where

$$F = \sqrt{W} - \sqrt{\zeta} + \rho \cos\theta \cdot \ln \frac{\sqrt{W} + h(z') - \rho \cos\theta}{\sqrt{\zeta} - \rho \cos\theta} \tag{37}$$

$$W = G^2 + (z - z')^2 + \rho^2 + h^2(z') - 2\rho h(z') \cos\theta \tag{38}$$

$$\zeta = G^2 + \rho^2 + (z - z')^2 \tag{39}$$

$$\theta = \phi - \phi'. \tag{40}$$

The remaining integrations can be carried out numerically by computer. The calculated $H(L)$ for $G = 0.75$, 1.5, and 3 km, respectively, are shown in Fig. 4.

Notice that the radius $h(z)$ of a "radio beam cross section" is on the order of several meters, whereas the characteristic distance G is on the order of kilometers (see Section 4.1). Therefore,

$$G \gg h(z) \tag{41}$$

for most radio paths at frequencies above 10 GHz. Imposing the condition (41) reduces the complicated integrations in eq. (36) to the simple result

$$H(L) \cong \frac{2G^2}{L^2} \left\{ \frac{L}{G} \ln \left[\frac{L}{G} + \sqrt{1 + \frac{L^2}{G^2}} \right] - \sqrt{1 + \frac{L^2}{G^2}} + 1 \right\}. \tag{42}$$

The differences in numerical values of $H(L)$ calculated by (36) and by approximation (42) are less than 0.1 percent within the range of interest. Notice that $H(L)$ is practically independent of wavelength

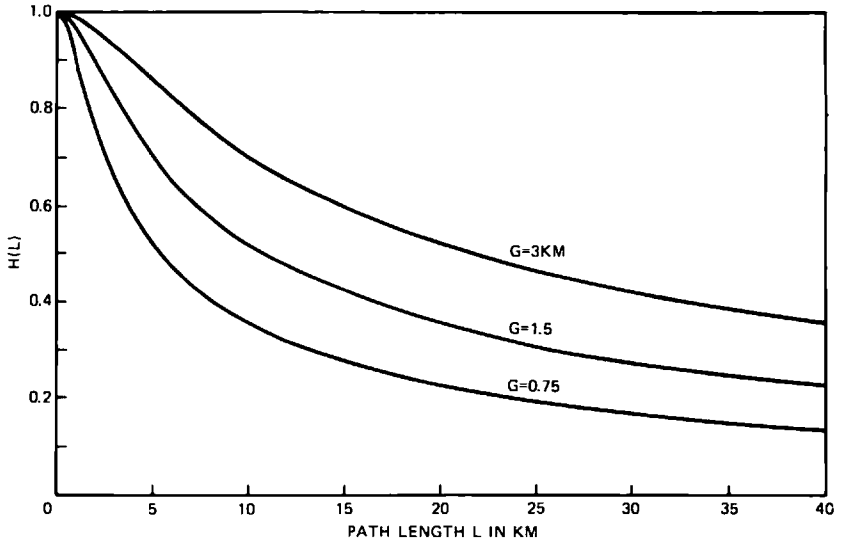

Fig. 4—Dependence of $H(L)$ on path length L and characteristic distance G.

λ because of condition (41). Therefore, we omit the wavelength specification on Fig. 4.

Thus, we have obtained all the necessary relationships. The procedure for calculating rain attenuation distributions from point rain rate distributions is summarized in the next section.

3.2 Procedure for calculating rain attenuation distribution

(*i*) Convert the measured distribution of point rain rate with $T \leqq 2$ min into the distribution of 2-s point rain rates by the conversion factor in Ref. 15.

(*ii*) If $P_0(0)$ with $T \leqq 1$ min is not available at the location of interest, use approximation (19) and the Weather Bureau hourly precipitation data to estimate P_0.

(*iii*) Estimate the lognormal parameters R_m and S_R of the 2-s point rain rate distribution by a least-squares approximation. This step is carried out by a computer iteration process to obtain the (R_m, S_R) pair that minimizes the differences (i.e., the sum of squares of errors) between the data points and the lognormal approximation.

(*iv*) Calculate β_m and S_β by formulas (15) and (16).

(*v*) Calculate $P_0(L)$, $\alpha_m(L)$, and $S_\alpha(L)$ by formulas (20), (30), and (31).

(*vi*) Substitute $P_0(L)$, $\alpha_m(L)$, $S_\alpha(L)$ into eq. (1) to give the attenuation distribution.

IV. COMPARISON OF CALCULATED RESULTS WITH EXPERIMENTAL DATA

The measured rain attenuations in many experiments contain not only the path rain attenuation but also the transmission loss owing to wet radomes. The presently available information is insufficient for *accurate* estimation of wet radome attenuation as a function of rain rate, wind direction, radome shape, size, material, and surface aging effects.

Based upon two measurements of wet radome attenuations discussed in Appendix D, we assume that a flat, vertical radome causes 1.5-dB attenuation during heavy rain. Therefore, 3-dB attenuation, caused by a pair of wet radomes, is added to the calculated path rain attenuation and the result is compared with the measured data utilizing such radomes. In some experiments, the flat radomes are slanted inward to further reduce wetting the radome surfaces. The attenuation caused by a pair of such radomes during rain is assumed* to be less than 3 dB. More detailed discussion of the radome problem is given in Appendix D.

4.1 Determination of characteristic distance G

From the 3-year (1971–1973) distribution of 1-min point rain rates measured at Merrimack Valley, Massachusetts,[36] the conversion factor in Ref. 15, and the Weather Bureau data,[32] we obtain the following approximate lognormal parameters of the distribution of 2-s point rain rate:

$$P_0(0) \simeq 3.3\%, \tag{43}$$

$$R_m \cong 1.23 \text{ mm/h}, \tag{44}$$

and

$$S_R \simeq 1.34. \tag{45}$$

Following the procedure outlined in Section 3.2, we use these parameters to calculate a family of rain attenuation distributions as a function of the distance parameter G. Figure 5 displays the results for an 18-GHz, 4.3-km path subject to Merrimack Valley rain and makes comparison with measured data (1971–1973) at the same location (Ref. 36 and Tables II and III). The radomes on this path are vertical and almost flat. The solid curves on Fig. 5 are calculated path rain attenuations plus assumed 3-dB radome attenuation. Figure 5 indicates that

$$G \cong 1.5 \text{ km} \tag{46}$$

provides good agreement; therefore, a 1.5-km characteristic distance[39,40]

* The slanted radomes may get wet during some heavy rains accompanied by strong wind gusts.

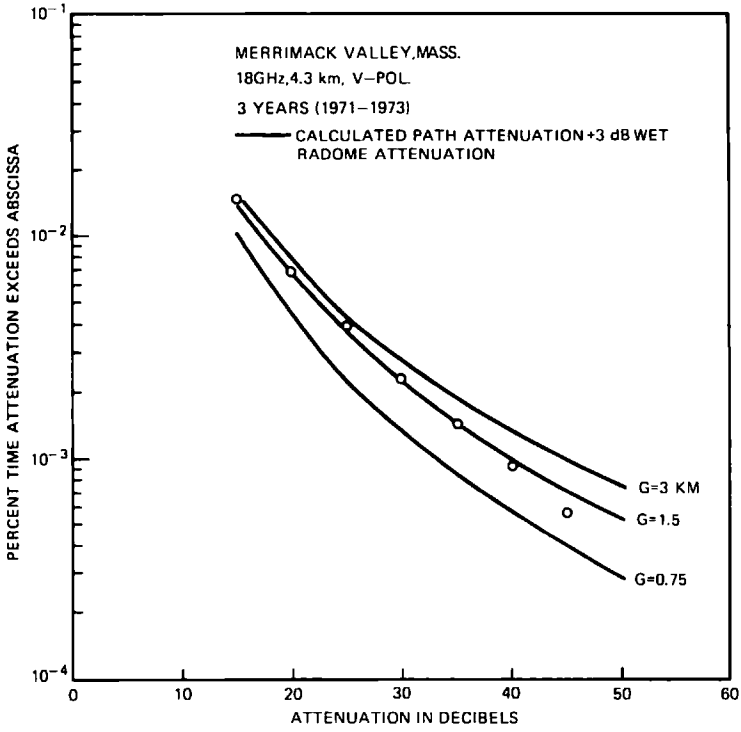

Fig. 5—Determination of characteristic distance G by comparing experimental data with calculated results (solid lines) using rain rate data in Fig. 10.

is used for the calculations and comparisons with other sets of data at other locations in the following sections.

From eqs. (35) and (46), it is easily shown that $d \leqq 15$ km for a spatial correlation coefficient, $\psi_u \geqq 0.1$. In other words, a "rain cell," based upon a definition of $\psi_u \geqq 0.1$ within the cell, has a typical spatial extent of 15 km. Obviously, the cell size depends on its definition.

4.2 Comparisons of calculated results with data in Georgia

Figure 6 compares the calculated result with data from a 5.1-km 17.7-GHz path at Palmetto, Georgia, measured during two 1-year periods (November 1970 through October 1971 and August 1973 through July 1974).* The radomes on this path are flat and canted inward. The calculated result is based upon the rain rate distribution measured by a tipping-bucket rain gauge at Palmetto in the same time

* The data from November 1971 to July 1973 are not used because of intermittent troubles in the rain gauge and the magnetic tape recorder.

Table II — Experimental data on rain attenuation distribution

No.	Authors	Ref No.	Freq (GHz)	Path Length (km)	Polarization	Fig. No.	Path Location	Time Base	Radome Shape Orientation	Rain Rate Data Used in Theoretical Calculation
1	Barnett, Bergmann, Lin, Pursley	30, 37	17.7	5.1	H	6	Rico-Palmetto, Ga.	11/70–10/71 8/73–7/74	Flat, slanted	No. 5 of Table 2
2	Pursley	37	11.6	42.	V	7	Atlanta-Palmetto, Ga.	8/73–7/74	Flat, almost vertical	No. 6 of Table 2
3	Lentz, Kenny	36	18.4	4.3	V	5	Merrimack Valley, Mass.	1971–1973	Flat, vertical	No. 7 of Table 2
4	Semplak	38	18.5	6.4	V	8	Holmdel, N.J.	1968–1969	Flat, slanted*	No. 8 of Table 2

* These radomes are shrouded by wooden rain shields.

Table III — Experimental data on point rain rate distribution

No.	Authors	Ref No.	Fig. No.	Location	Time Base	Rain Gauge Integration Time	Rain Gauge	Estimated Lognormal Parameters		
								Rm mm/hr	S_R	$P_0(0)$
1	Ruthroff, Bodtmann	15	11	Miami, Fla	1966–1970	1 min	Weighing Gauge	2.48	1.54	0.026
2	Jones, Sims	14, 20	11	Miami, Fla	8/57–8/58	1 min	Weighing Gauge	2.48	1.54	0.026
3	Jones, Sims	14, 20	10	Urbana, Ill	5/69–4/72	1 min	Weighing Gauge	1.1	1.47	0.033
4	Ruthroff, Bodtmann, Osborne	15	12	Atlanta, Ga.	1966–1970, 1973	1 min	Weighing Gauge	3.23	1.15	0.026
5	Lin		12	Palmetto, Ga.	11/70–10/71 8/73–7/74	1 min	Tipping Bucket	3.10	1.18	0.031
6	Lin		13	Palmetto, Ga.	8/73–7/74	1 min	Tipping Bucket	3.85	1.11	0.030
7	Lentz	36	10	Merrimack Valley, Mass.	1971–1973	10–90 s	Ruthroff's (Ref 2)	1.23	1.34	0.033
8	*		11	Holmdel, N.J.*	1968–1969	2 s	*	1.53	1.38	0.026
9	Norbury, White	16	10	Slough, England	1970–1971	10 s to 1 h	Special Dropper Gauge	0.42	1.4	0.044
10	Easterbrook, Turner	17	10	Southern England	5/61–5/62 1963	2–60 min	?			

* Point rain rate distribution from 1968 to 1969 at Holmdel, New Jersey, is estimated from rain attenuation data on short paths at Holmdel. See Section 4.3.

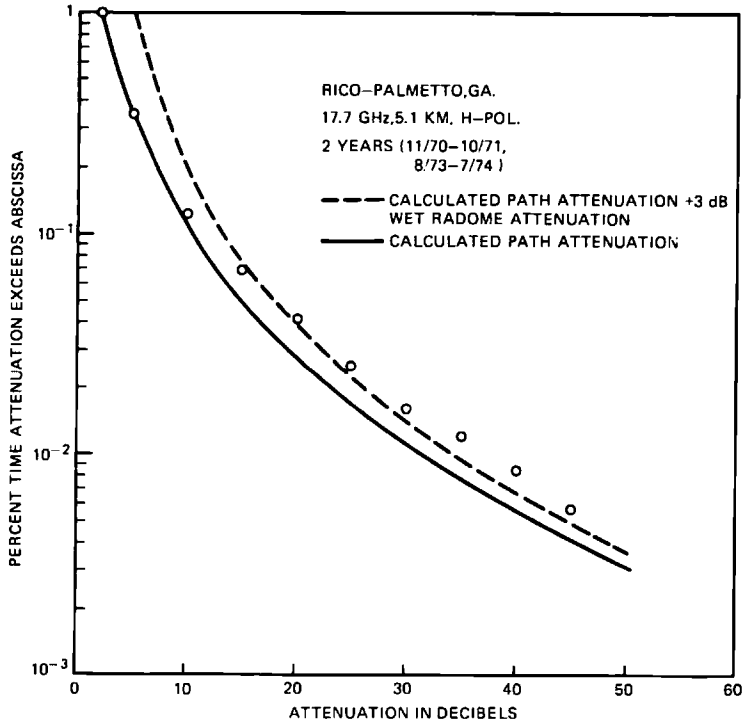

Fig. 6—Comparison of 17.7-GHz rain attenuation data at Palmetto, Georgia, with calculated result (solid line) using rain rate data in Fig. 12.

period. Figure 6 has two calculated attenuation curves, one without radome attenuation and another with 3-dB radome attenuation.

In the 11-GHz band, the path lengths of interest may be as long as 50 km. It is desirable to test the validity of the method for long paths. A preliminary comparison is shown in Fig. 7 for an 11-GHz, 42-km path between Atlanta and Palmetto, Georgia. The radomes on this path are flat and almost vertical. The attenuation and rain rate were observed during a 1-year period (August 1973 through July 1974). The calculated-plus-3-dB-radome-loss result is reasonably close to the data. In Figs. 7 and 13, notice that the measured attenuation and rain rate distributions are both somewhat higher than the lognormal approximations in the probability range from 10^{-2} to 4×10^{-2} percent time. We believe that these deviations are an artifact of the short observation time. A more critical test of this method for long paths awaits longer-term data.

4.3 Comparison of calculated result with data in New Jersey

Rain attenuation experiments on two paths (18 GHz, 6.4 km, and 30.9 GHz, 1.9 km) were carried out simultaneously in 1968 and 1969 at Holmdel, New Jersey.[38] However, local point rain rate distributions were not measured during this period. On the other hand, Bodtmann and Ruthroff[15] have suggested a method for relating point rain rate distribution to path rain attenuation distributions on short paths. Thus, by using the short-path attenuation data from the 30.9-GHz, 1.9-km path and Bodtmann and Ruthroff's method, the 2-year distribution of point rain rate at Holmdel was estimated as shown in Fig. 11. Based on this estimated rain rate distribution, we calculate the 2-year rain attenuation distribution on an 18-GHz, 6.4-km path and compare this with the measured result in Fig. 8. The radomes in these experiments are flat, slanted inward, and shrouded by substantial wooden rain shields. We believe that the wet radome attenuation, with

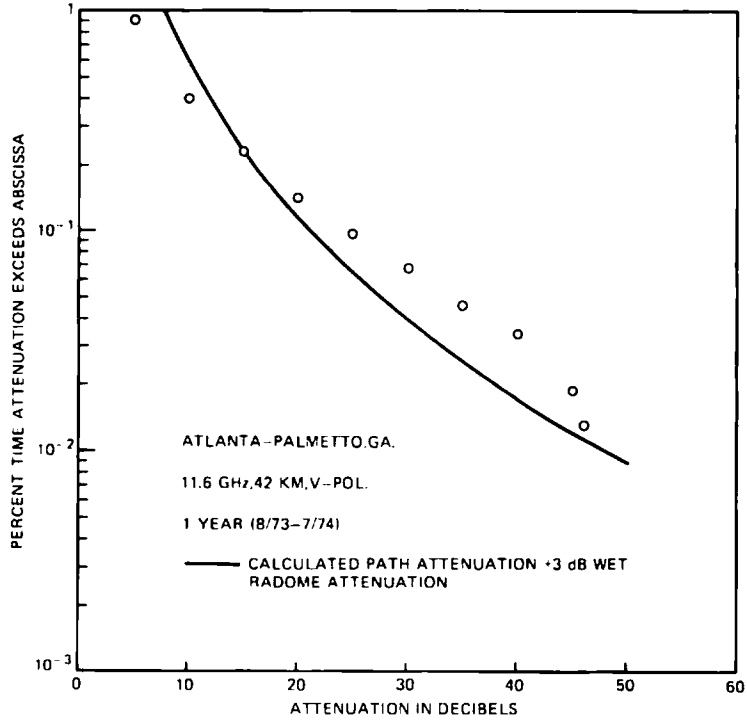

Fig. 7—Preliminary comparison of 1-year rain attenuation data from an 11-GHz, 42-km path in Georgia with calculated results (solid line) using rain rate data in Fig. 13.

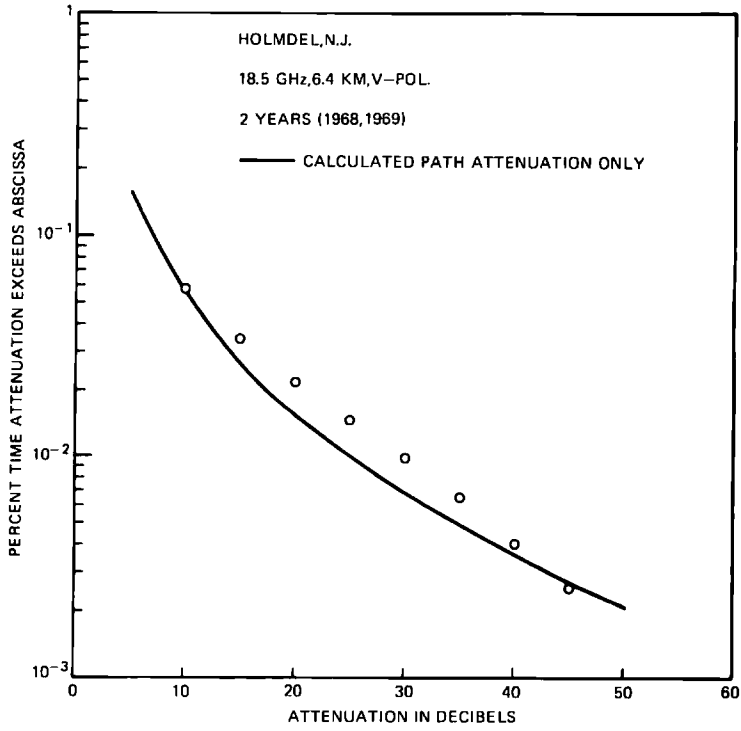

Fig. 8—Comparison of 18.5-GHz rain attenuation data in Holmdel, New Jersey, with calculated result (solid line) using rain rate data in Fig. 11.

such protection, is negligible. Therefore, the calculated curve in Fig. 8 contains only path rain attenuation.

Figures 6, 7, and 8 show that the calculated results agree reasonably well with measured data.

4.4 Excluded rain attenuation data

Many sets of rain attenuation data in the literature are not included in the comparisons in Sections 4.2 and 4.3 because of one or more of the following reasons.

(*i*) Many experiments used cone-shaped or hemispheric-shaped radomes. The transmission loss resulting from rain running on a pair of such radomes may vary from 0 to 14 dB depending on frequency, rain rate, and radome surface aging. The uncertainty in estimating such radome attenuation is too large for a meaningful comparison between the data and the calculated path rain attenuation distribution.

(*ii*) The antennas in the experiment are not covered by any radomes, exposing the antenna feeds and reflecting surfaces to rain, snow, and ice. No information is available for estimating the possible transmission loss from the wetting of these elements.

(*iii*) The published information does not specify whether the antennas are covered by radomes or not. The configuration of the radome, if used, is also unknown.

(*iv*) The polarization of the transmitted signal is unstated.

(*v*) The time base of the experiment is too short to yield long-term representative statistics.

(*vi*) No rain rate data with $T \leqq 2$ min is available at or near the location of the rain attenuation experiment.

V. OUTAGE ESTIMATION FOR 11- AND 18-GHz RADIO LINKS

For a constant transmitter output power, the dependence of fade margin $F_0(L)$ in dB on the path length L is

$$F_0(L) = F_0(L_0) - 20 \log_{10}\left(\frac{L}{L_0}\right) \text{dB}, \tag{47}$$

where L_0 is a reference repeater spacing and $F_0(L_0)$ is the corresponding reference fade margin. For 11- and 18-GHz radio, reasonable clear-day reference fade margins are

$$F_0 = 40 \text{ dB for 18 GHz at } L_0 = 4 \text{ km}$$

and

$$F_0 = 40 \text{ dB for 11 GHz at } L_0 = 40 \text{ km}.$$

A radio outage occurs when the path rain attenuation plus the wet radome attenuation exceeds the clear-day fade margin F_0. By substituting the fade margin (47) into the attenuation distribution (1), we can calculate the probability of radio outage per hop as a function of repeater spacing L. As an example, Fig. 9 shows the outage probabilities* for 11- and 18-GHz radio links in Atlanta, Georgia.

The wet radome attenuation A_R is assumed to be 3 dB in these calculations of outage probabilities.

VI. SOME QUALIFICATIONS

This section discusses some limitations, approximations, and assumptions in the theoretical calculation procedure, the data employed, and the calculated results.

---

* Multipath interference fading can also cause outages. An empirical formula for estimating the multipath-caused outage probability can be found in Ref. 41.

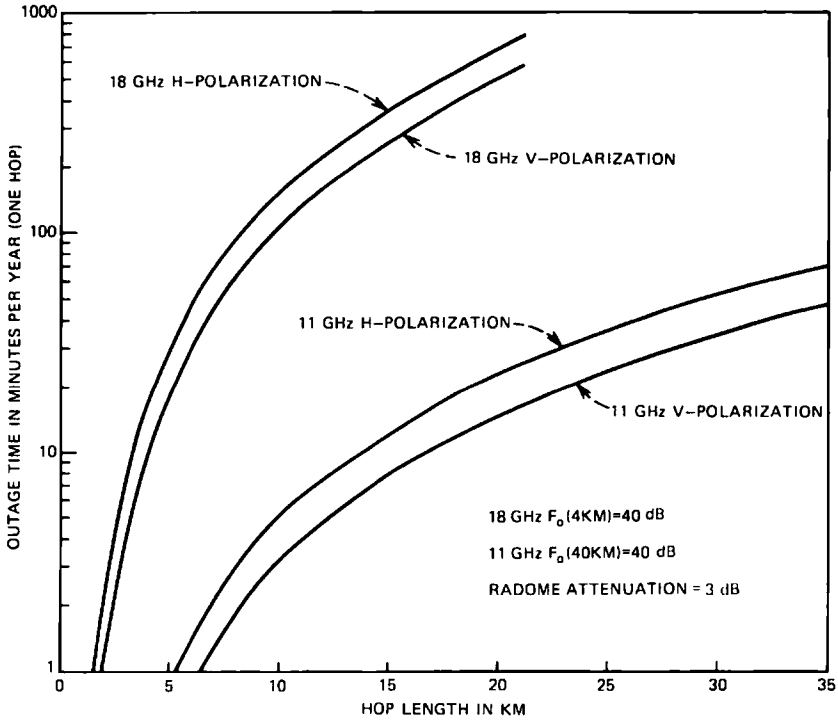

Fig. 9—Expected outage times of 11- and 18-GHz radio links as a function of hop length in Atlanta, Georgia.

6.1 Uncertainty in estimation of lognormal parameters P_0, R_m, and S_R

Some point rain rate measurements report only the heavy rain (e.g., $\geqq 30$ mm/h) portion of the distribution, neglecting the light rain statistics completely. Table III indicates that the median rain rates R_m at many locations are less than 4 mm/h. In other words, the major portion ($\cong$98 percent) of the distribution is missing, and accurate estimation of the statistical parameters R_m and S_R from the tail region ($\leqq 2$ percent) is difficult.

Furthermore, high rain rates (e.g., >140 mm/h) require a long observation time to yield representative, long-term statistics. The time bases of most available data may not be sufficient to yield stable statistics for these extreme rain rates. For example, at Newark, New Jersey, the 1-min point rain rate exceeded 180 mm/h *only once* in the 5-year period processed by Bodtmann and Ruthroff. To obtain reasonably stable statistics, we need a sample size much larger than 1. The omission of light-rain statistics together with the inherent instability of the extreme rain rate statistics causes considerable un-

certainty in the estimation of P_0, R_m, and S_R. This uncertainty can be reduced significantly if the light rain portion of the distribution is also measured and reported.

6.2 Path length dependence of P_0

The empirical formula (20) for the dependence of P_0 on path length L is obtained from the rain-gauge network data in Florida. The test of the applicability of this empirical formula to other locations and the improvement of this approximation will require further multiple rain gauge experiments at other locations.

6.3 Dependence of point rain rate distribution on rain gauge integration time

The dependence of the point rain rate distribution on rain-gauge integration time T has been obtained by Bodtmann and Ruthroff[15] from a 2-year experiment at Holmdel, New Jersey. Since a 2-year time base may not be sufficient to yield stable statistics for high rain rates, a longer time base may be needed to improve this empirical conversion factor. The applicability of this result to other geographic locations also remains to be verified.

6.4 Radome problem

In the comparisons of calculated and measured rain attenuation distributions, the wet radome attenuations are assumed values. To improve this approximation, a more systematic experimental study on the dependence of radome attenuation on rain rate is needed.

6.5 Anisotropic spatial correlation ψ

At some geographic locations, the squall lines of heavy rain may have a predominant orientation related to the predominant orientation of weather fronts.[42–44] This means the spatial correlation ψ may depend not only on the spacing but also on the orientation. However, the presently available information is not sufficient for a *quantitative* description of such an anisotropic correlation. Therefore, we use the isotropic correlation coefficient (35) throughout our theoretical calculations. Some of the difference between calculated and measured attenuation distributions may be caused by neglecting the anisotropy of the spatial correlation function.

VII. CONCLUSION

By using lognormal approximations, we have described a method for calculating rain attenuation distributions on microwave paths. The calculated results agree reasonably well with experimental data in Massachusetts, New Jersey, and Georgia. This procedure may

prove useful for the design of radio paths using frequencies above 10 GHz. To demonstrate the application, Fig. 9 shows the calculated outage probability as a function of repeater spacing for 11- and 18-GHz radio links in Georgia.

VIII. ACKNOWLEDGMENTS

I wish to express appreciation to K. A. Jarett who has helped in developing a computer program for the numerical calculations in this paper; to N. Levine, E. E. Muller, W. T. Barnett, D. C. Hogg, A. A. M. Saleh, and T. S. Chu for valuable comments and suggestions that greatly improved the consistency and precision of this analysis; to D. C. Hogg, R. A. Semplak, R. A. Desmond, A. E. Freeny, and J. D. Gabbe for rain rate and attenuation data at Holmdel; to W. T. Barnett, M. V. Pursley, and H. J. Bergmann for attenuation data in Georgia; to G. H. Lentz and J. J. Kenny for rain rate and attenuation data in Massachusetts; and to C. L. Ruthroff, W. F. Bodtmann, and A. L. Sims for rain rate data at many locations.

APPENDIX A

Derivation of Formulas Relating Rain Attenuation Distribution to Path Length

Since the random fluctuations of the attenuation gradient $\beta(\mathbf{s})$ at various positions in the radio path are partially correlated, we require the spatial covariance function of β to relate the variance of β to the variance of the path attenuation α. However, raining intervals at separated observation points are not always coincident. Hence, definition of the spatial covariance function for β requires a time base for all βs common to all observations. A natural common time base fulfilling this requirement is the total time, including both raining and nonraining intervals. This means the unconditional* statistical means and variances of β and α are also needed in this formulation. We therefore define

$$\bar{\beta}_u = E_u\{\beta(t)\} \tag{48}$$

and

$$\sigma_{\beta u}^2 = E_u\{\beta^2(t)\} - \bar{\beta}_u^2 \tag{49}$$

as the unconditional mean and variance, respectively, of β, where $E_u\{\sim\}$ denotes the (unconditional) statistical average including both raining and nonraining time. We assume that, on a long-term basis, $\bar{\beta}_u$ and $\sigma_{\beta u}^2$ are independent of position in or near the radio path of

* Fading caused by other atmospheric effects, such as multipath interference and "earth-bulge," is not treated in this paper. Therefore, the path rain attenuation α and the attenuation gradient β are taken to be identically zero during nonraining time.

interest; therefore, we omit the position argument(s) in eqs. (48) and (49). Similarly,

$$\bar{\alpha}_u = E_u\{\alpha(t)\} \tag{50}$$

$$\sigma^2_{\alpha u} = E_u\{\alpha^2(t)\} - \bar{\alpha}^2_u \tag{51}$$

are the unconditional mean and variance, respectively, of α.

Based upon the definitions (48) to (51) and the relationships (22) to (29), it can be shown that conditional and unconditional means and variances are related by

$$\bar{\beta} = \bar{\beta}_u / P_0(0) \tag{52}$$

$$\bar{\alpha} = \bar{\alpha}_u / P_0(L) \tag{53}$$

$$S^2_\beta = \ln\left\{P_0(0)\left[1 + \frac{\sigma^2_{\beta u}}{\bar{\beta}^2_u}\right]\right\} \tag{54}$$

and

$$S^2_\alpha = \ln\left\{P_0(L)\left[1 + \frac{\sigma^2_{\alpha u}}{\bar{\alpha}^2_u}\right]\right\}. \tag{55}$$

Obtaining the unconditional statistical averages of both sides of eq. (6) yields

$$\bar{\alpha}_u = \bar{\beta}_u \cdot L. \tag{56}$$

Substituting eqs. (6) and (56) into definition (51) yields

$$\begin{aligned}\sigma^2_{\alpha u} &= E_u\left\{\int_0^L \frac{1}{Q(z)} \int_{Q(z)} \int\int_0^L \frac{1}{Q(z')} \right. \\ &\qquad \left. \times \int_{Q(z')} \int \beta(\mathbf{s}, t)\cdot\beta(\mathbf{s}', t)\cdot dv dv'\right\} - \bar{\beta}^2_u \cdot L^2 \\ &= \int_0^L \frac{1}{Q(z)} \int_{Q(z)} \int\int_0^L \frac{1}{Q(z')} \\ &\qquad \times \int_{Q(z')} \int \{E_u[\beta(\mathbf{s}, t)\cdot\beta(\mathbf{s}', t)] - \bar{\beta}^2_u\}\cdot dv dv'. \end{aligned} \tag{57}$$

Let us define a spatial covariance function[34,35] $C_\beta(\mathbf{s}, \mathbf{s}')$ for $\beta(\mathbf{s}, t)$ and $\beta(\mathbf{s}', t)$ such that

$$C_\beta(\mathbf{s}, \mathbf{s}') = E_u\{\beta(\mathbf{s}, t)\cdot\beta(\mathbf{s}', t)\} - \bar{\beta}^2_u. \tag{58}$$

In other words,

$$\psi_u(\mathbf{s}, \mathbf{s}') = \frac{C_\beta(\mathbf{s}, \mathbf{s}')}{\sigma^2_{\beta u}} \tag{59}$$

is the (spatial) correlation coefficient[34,35] between $\beta(\mathbf{s}, t)$ and $\beta(\mathbf{s}', t)$. Substituting definitions (58) and (59) into (57) yields

$$\sigma^2_{\alpha u} = \sigma^2_{\beta u} \cdot L^2 \cdot H(L), \tag{60}$$

where

$$H(L) = \frac{1}{L^2}\int_0^L \frac{1}{Q(z)}\int_{Q(z)}\int\int_0^L \frac{1}{Q(z')}\int_{Q(z')}\int \psi_u(\mathbf{s}, \mathbf{s}')dvdv'. \quad (61)$$

Substituting (56) and (60) into (55) gives

$$S_\alpha^2(L) = \ln P_0(L)\cdot\left[1 + H(L)\cdot\frac{\sigma_{\beta u}^2}{\bar{\beta}_u^2}\right]. \quad (62)$$

Combining (54) and (62) gives

$$S_\alpha^2(L) = \ln P_0(L)\cdot\left\{1 + H(L)\left[\frac{\exp(S_\beta^2)}{P_0(0)} - 1\right]\right\}. \quad (63)$$

Combining eqs. (24), (25), (52), (53), and (56) gives

$$\alpha_m(L) = \beta_m\cdot L\cdot\frac{P_0(0)}{P_0(L)}\cdot\exp\left[\frac{S_\beta^2 - S_\alpha^2}{2}\right]. \quad (64)$$

This completes the derivation for $S_\alpha^2(L)$ and $\alpha_m(L)$.

APPENDIX B

Lognormal Distribution of Point Rain Rate

Figures 10 to 13 display the distributions of 2-s point rain rate observed in Miami, Florida; Urbana, Illinois; Atlanta and Palmetto, Georgia; Merrimack Valley, Massachusetts; Holmdel, New Jersey; and Southern England. The time bases range from 1 to 6 years. It can be seen that these distributions of 2-s point rain rate are very close to the lognormal approximation in the range below 100 mm/h. The rain rates beyond 100 mm/h are generally separated by more than 3 sigma from the median, and constitute the tail of the lognormal distribution. A very long observation time (e.g., more than 20 years) is necessary to obtain stable statistics of extreme rain rates beyond 100 mm/h.[45–48] Since the time bases of the data in Figs. 10 to 13 are much less than 20 years, the deviations of the data from the lognormal distributions in the tails are not unexpected.

The rain gauge integration time T in the original data range from 1.5 s to 2 min, depending upon the source. As discussed in Section 2.3, the appropriate integration time T, corresponding to 1-m^3 sampling volume in our formulation, is about 2 s. From 2-year experimental data at Holmdel, New Jersey, Bodtmann and Ruthroff[15] have obtained an empirical relationship for the dependence of point rain rate distributions on rain gauge integration t time in the range

$$1.5\text{ s} \leqq T \leqq 120\text{ s}. \quad (65)$$

This empirical result enables us to convert the original data into the 2-s point rain rate distributions shown in Figs. 10 to 13.

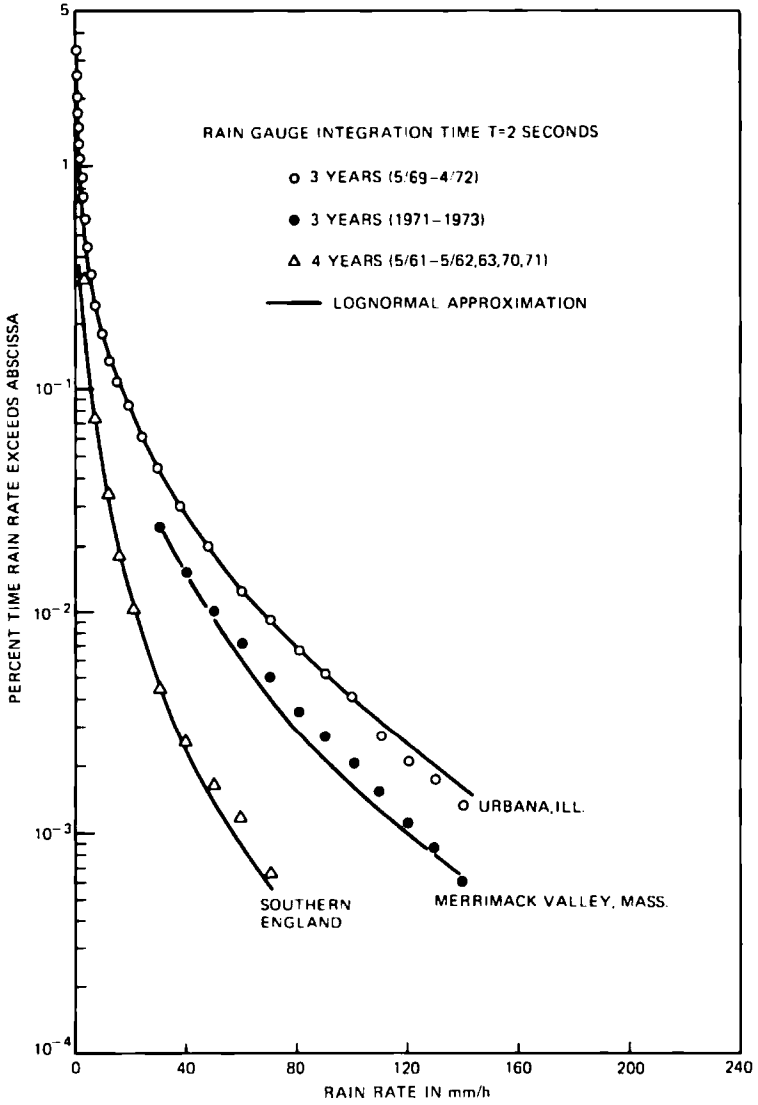

Fig. 10—Lognormal distribution of 2-s point rain rate at Urbana, Illinois; Merrimack Valley, Massachusetts; and Southern England.

APPENDIX C

Derivation for Path Length Dependence of $P_0(L)$

Let $P_0(L_1)$ and $P_0(L_1 + \Delta L)$ be the probabilities that rain falls on the radio path with length L_1 and an extended path of length $L_1 + \Delta L$, where ΔL is a small incremental length. The relation between $P_0(L_1)$

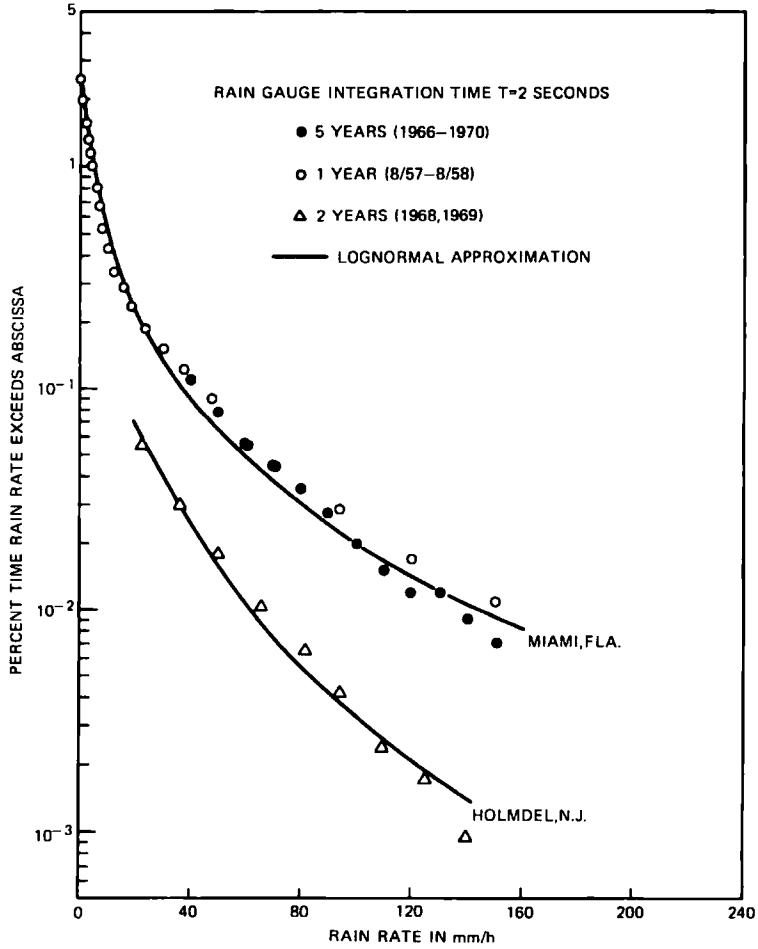

Fig. 11—Lognormal distribution of 2-s point rain rate at Miami, Florida and Holmdel, New Jersey.

and $P_0(L_1 + \Delta L)$ can be written as

$$P_0(L_1 + \Delta L) = P_0(L_1) + \Delta P_0(\Delta L), \tag{66}$$

where $\Delta P_0(\Delta L)$ is the incremental probability of rainfall associated with the incremental length ΔL. This incremental probability can be written as

$$\Delta P_0(\Delta L) = \Delta P_0(\Delta L | \text{no rain for } 0 \leqq L \leqq L_1) \cdot P(\text{no rain for } 0 \leqq L \leqq L_1), \tag{67}$$

where $\Delta P_0(\Delta L | \text{no rain for } 0 \leqq L \leqq L_1)$ is the (incremental) probability that rain falls on the incremental length ΔL under the condi-

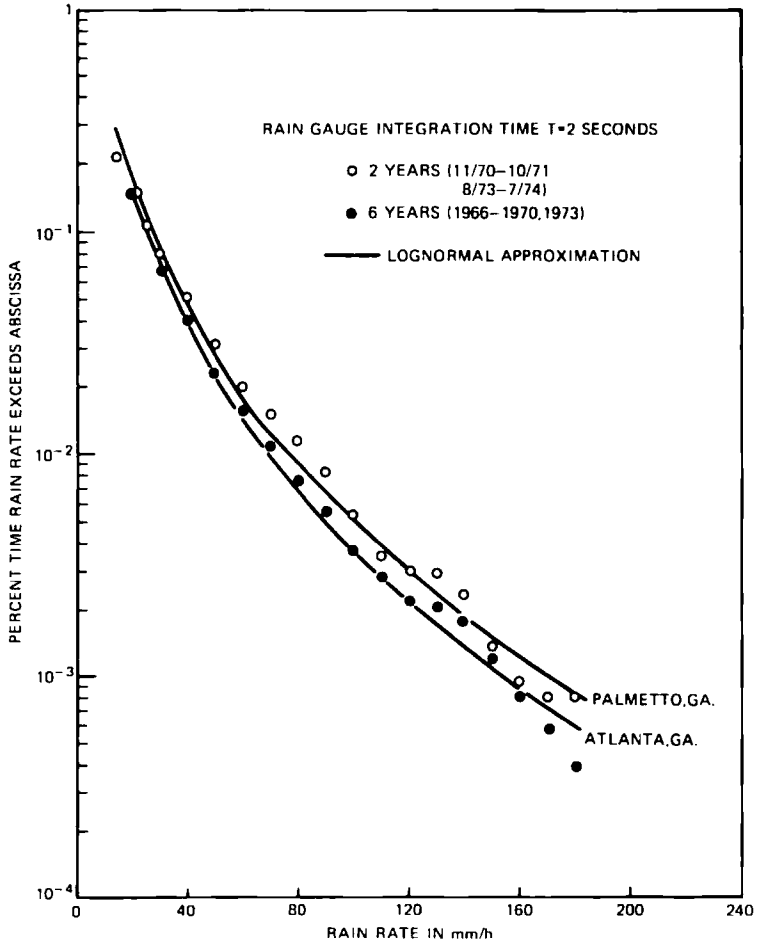

Fig. 12—Lognormal distribution of 2-s point rain rate at Palmetto and Atlanta, Georgia.

tion that rain is not falling on the path L_1. This condition is required because rainfall on L_1 and ΔL are partially correlated.

We assume that

$$\Delta P_0(\Delta L \,|\, \text{no rain for } 0 \leqq L \leqq L_1) \propto \Delta L. \tag{68}$$

The justification for this assumption is

(*i*) $P_0(L)$ is expected to be a smooth, continuous function of L, i.e.,

$$\lim_{\Delta L \to 0} P_0(L_1 + \Delta L) = P_0(L_1), \tag{69}$$

$$\lim_{\Delta L \to 0} \Delta P_0(\Delta L \,|\, \text{no rain for } 0 \leqq L \leqq L_1) = 0. \tag{70}$$

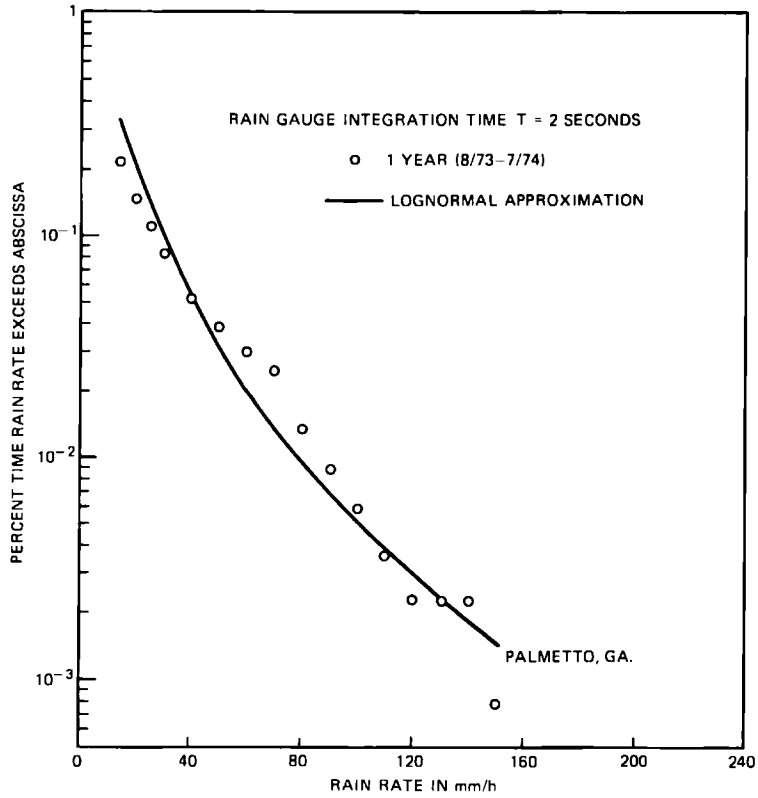

Fig. 13—Lognormal distribution of 2-s point rain rate at Palmetto, Georgia.

(*ii*) The rain-gauge network data (Fig. 3) indicate that the slope of $P_0(L)$ is not zero, i.e.,

$$\frac{\Delta P_0}{\Delta L} \neq 0, \qquad \text{for } L \neq 0.$$

Let b be the proportional parameter in assumption (68). Then

$$\Delta P_0(\Delta L \,|\, \text{no rain for } 0 \leqq L \leqq L_1) = b(L) \cdot \Delta L. \tag{71}$$

The unknown proportional parameter $b(L)$ will be determined from rain-gauge network data.

By definition,

$$P(\text{no rain for } 0 \leqq L \leqq L_1) = 1 - P_0(L_1). \tag{72}$$

Combining eqs. (67), (71), and (72) yields

$$\Delta P_0(\Delta L) = b(L) \cdot \Delta L \cdot [1 - P_0(L_1)], \tag{73}$$

from which

$$\frac{dP_0(L)/dL}{1 - P_0(L)} = b(L). \tag{74}$$

Integrating (74) yields

$$P_0(L) = 1 - c \exp\left\{-\int_0^L b(z)dz\right\}, \tag{75}$$

where c is an unknown constant to be determined by the condition

$$\lim_{L \to 0} P_0(L) = P_0(0). \tag{76}$$

Applying condition (76) to (75) gives

$$P_0(L) = 1 - [1 - P_0(0)] \exp\left\{-\int_0^L b(z)dz\right\}. \tag{77}$$

Since the rain-gauge network data yield $P_0(L)$ at only a few discrete distances, we need the quantized version

$$\frac{\Delta P_0(L_i)/\Delta L}{1 - P_0(L_i)} \cong b(L_i), \qquad i = 1, 2, 3, \cdots, n, \tag{78}$$

of eq. (74) for estimating $b(L)$. By using eq. (78) and the rain-gauge network data in Fig. 3, we can calculate $b(L_i)$ at several discrete points. From these results, we find that $b(L)$ can be approximately described by the empirical formula

$$b(L) \cong \frac{0.028L}{21.5 + L^2} \text{ (km}^{-1}\text{)}. \tag{79}$$

Substituting (79) into (77) and carrying out the integration yields

$$P_0(L) \cong 1 - \frac{1 - P_0(0)}{\left[1 + \dfrac{L^2}{21.5}\right]^{0.014}}, \tag{80}$$

which is the same as (20).

Figure 3 shows that the empirical result (80) is reasonably close to all the data points measured by the Florida rain-gauge network. Admittedly, eqs. (79) and (80) are empirical. Further theoretical work and multiple rain-gauge experiments are needed to improve these approximations.

APPENDIX D

Transmission Loss Due to Wet Radomes

A 20-GHz experiment by Anderson[49] on a section of a 90-ft diameter radome, pertaining to an earth satellite radio link, indicated a transmission loss of 2 to 3 dB at 10 mm/h rain rate when the radome

was new. However, after 6 months of weathering, the transmission loss increased to 8 dB at 10 mm/h rain rate. A 4-GHz experiment[50] on an earth-satellite radio link indicated a 3-dB transmission loss resulting from the wet radome. These experimental data agree reasonably well with theoretical calculations[51–54] for rain rates $\leqq 10$ mm/h, assuming laminar water flow on hemispherical radome surface pointing towards the zenith.

For typical 11- and 18-GHz terrestrial radio paths, the transmission losses from wet radomes are expected to be smaller than those of earth-satellite radio links because of the smaller radome size, different radome shape, and orientation. However, the terrestrial radio passes through a pair of radomes on each link; therefore, the contribution of wet radome loss to the total path attenuation may not be negligible. Theoretical calculation of wet radome attenuation pertaining to terrestrial radio links is not available at the present time because of the difficulty in calculating the nonuniform thickness of the water film. A semiquantitative experiment[55] was carried out on the 12.2-GHz radio link between Murray Hill and Crawford Hill, New Jersey (22 miles). The 10-ft dish antenna was covered by a cone-shaped radome that was made of resin-coated fiberglass and, at 10 years of age, was well weathered. Water was sprayed on the radome-covered antenna by a manually controlled sprinkler. The results indicated that a uniform light sprinkle caused approximately 2.5-dB attenuation, whereas a very heavy spray (maximum stream of water) caused between 4- and 7-dB attenuation. After the spray was turned off, 2 to 3 minutes elapsed before the signal recovered to within 1 dB of its nonfaded level. The residual wet radome attenuation is estimated to be 0.5 dB.

On an 18-GHz, 4.3-km path at Merrimack Valley, Massachusetts, Kenny[36] has also observed a residual wet radome attenuation of 0.75 dB (i.e., 1.5 dB for two radomes).

APPENDIX E

List of Symbols and Their Definitions

A_g	Collecting aperture of a rain gauge.
A_R	Attenuation by two wet radomes on a radio link.
$C_\beta(\mathbf{s}, \mathbf{s}')$	Spatial covariance function of $\beta(\mathbf{s}, t)$ and $\beta(\mathbf{s}', t)$ as defined by eq. (58).
dv	$= \rho d\rho d\phi dz$.
$E_L\{\sim\}$	Conditional statistical (time) average under the condition that the point rain rates, in the radio path of length L (see Fig. 1), are not all zero.

$E_0\{\sim\}$	Conditional statistical (time) average under the condition that the point rain rate (defined in Section 2.3) is not zero at the position of interest.
$E_u\{\sim\}$	Unconditional statistical (time) average including both raining and nonraining time.
erfc($\sim$)	Complementary error function.
F_0	Fade margin of radio links.
G	Characteristic distance defined in eq. (35). See also Section 4.1.
$h(z)$	Radius of the circular cross section of radio beam at a distance z from the transmitter. See Fig. 1 and eq. (3).
$H(L)$	Defined by eqs. (32) and (36).
H-Pol	Horizontal polarization.
L	The path length of a radio link; see Fig. 1.
L_0	A reference repeater spacing defined by eq. (47).
ln ($\sim$)	Natural logarithm.
$P(\alpha \geqq A)$	Probability that rain attenuation α exceeds A.
$P(R \geqq r)$	Probability that rain rate R exceeds r.
$P(\beta \geqq B)$	Probability that attenuation gradient β exceeds B.
$P_0(L)$	Probability that rain is falling on a radio link of length L.
$P_0(0)$	$= \lim_{L \to 0} P_0(L)$; the probability that rain is falling at the position of interest.
$Q(z)$	$= \pi h^2(z)$; area of the circular cross section of radio beam at a distance z from the transmitter. See eqs. (3) and (4).
$R(\mathbf{s}, t)$	Point rain rate measured by a 1-m^3 sampling volume located at $\mathbf{s}$.
R_m	Median value of the point rain rate R during raining time.
$\mathbf{s}$	A vector to denote the position (ρ, ϕ, z).
S_α	Standard deviation of ln α during raining time.
S_R	Standard deviation of ln R during raining time.
S_β	Standard deviation of ln β during raining time.
T	Integration time of rain gauge.
t	Time.
$T_{\Delta V}$	Defined in eq. (10).
V-Pol	Vertical polarization.
V_R	Average falling velocity of raindrops.
ΔV	Incremental sampling volume for measurement of point rain rate. See Section 2.3.
z	Distance from the radio transmitter (Fig. 1).
α	Rain attenuation in decibels.
α_m	Median value of α during raining time.
$\bar{\alpha}$	Mean value of α during raining time.

$\bar{\alpha}_u$	Unconditional statistical mean of α as defined by eq. (50).
β	Point rain attenuation gradient measured in dB/km by a 1-m^3 sampling volume as discussed in Section 2.3.
β_m	Median value of β during raining time.
$\bar{\beta}$	Mean value of β during raining time.
$\beta_Q(z, t)$	Average of $\beta(\mathbf{s}, t)$ over the circular cross section Q of the radio beam. See eqs. (5) and (7).
$\bar{\beta}_u$	Unconditional statistical mean of β as defined by eq. (48).
θ	$= \phi - \phi'$.
γ	A parameter defined by eq. (12) relating point rain attenuation gradient β and point rain rate R.
λ	Radio wavelength.
η	A parameter defined by eq. (12) relating point rain attenuation gradient β and point rain rate R.
σ_α	Standard deviation of α during raining time.
$\sigma_{\alpha u}$	Unconditional standard deviation of α as defined by eq. (51).
σ_β	Standard deviation of β during raining time.
$\sigma_{\beta u}$	Unconditional standard deviation of β as defined by eq. (49).
ρ	Radial distance from the z-axis in the cylindrical coordinate system in Fig. 1.
ϕ	Angle in the cylindrical coordinate system in Fig. 1.
$\psi_u(\mathbf{s}, \mathbf{s}')$	Correlation coefficient between $\beta(\mathbf{s}, t)$ and $\beta(\mathbf{s}', t)$ as defined by eqs. (33) and (59).

REFERENCES

1. A. E. Freeny and J. D. Gabbe, "A Statistical Description of Intense Rainfall," B.S.T.J., *48*, No. 6 (July–August 1969), pp. 1789–1851.
2. A. E. Freeny and J. D. Gabbe, private communication.
3. D. C. Hogg, "Statistics on Attenuation of Microwaves by Intense Rain," B.S.T.J., *48*, No. 9 (November 1969), pp. 2949–2962.
4. C. R. Stracca, "Propagation Tests of 11 GHz and 18 GHz on Two Paths of Difference Length," Alta Frequenza, Italy, *38*, 1969, pp. 345–360.
5. D. C. Hogg, "Path Diversity in Propagation of Millimeter Waves Through Rain," IEEE Trans. Ant. Prop., *AP-15*, No. 3 (May 1967), pp. 410–415.
6. S. H. Lin, "Statistical Behavior of Rain Attenuation," B.S.T.J., *52*, No. 4 (April 1973), pp. 557–581.
7. J. A. Morrison, M. J. Cross, and T. S. Chu, "Rain-Induced Differential Attenuation and Differential Phase Shift at Microwave Frequencies," B.S.T.J., *52*, No. 4 (April 1973), pp. 599–604.
8. T. Oguchi, "Attenuation and Phase Rotation of Radio Waves due to Rain: Calculation at 19.3 and 34.8 GHz," Radio Science, *8*, No. 1 (January 1973), pp. 31–38.
9. R. G. Medhurst, "Rainfall Attenuation of Centimeter Waves: Comparison of Theory and Measurement," IEEE Trans. Ant. Prop., *AP-13*, No. 4 (July 1965), pp. 550–564.
10. D. E. Setzer, "Computed Transmission Through Rain at Microwave and Visible Frequencies," B.S.T.J., *49*, No. 8 (October 1970), pp. 1873–1892.

11. J. W. Ryde, "Echo Intensity and Attenuation due to Clouds, Rain, Hail; Sand and Dust Storms at Centimeter Wavelength," Report 7831, General Electric Company Research Laboratories, Wembly, England, October 1941.
12. D. Ryde and J. W. Ryde, "Attenuation of Centimeter Waves by Rain, Hail and Clouds," Report 8516, General Electric Company Research Laboratories, Wembly, England, August 1944.
13. D. Ryde and J. W. Ryde, "Attenuation of Centimeter and Millimeter Waves by Rain, Hail, Fogs and Clouds," Report 8670, General Electric Company Research Laboratories, Wembly, England, May 1945.
14. D. M. A. Jones and A. L. Sims, "Climatology of Instantaneous Precipitation Rates," Illinois State Water Survey at the University of Illinois, Urbana, Illinois. Project No. 8624, Final Report, December 1971.
15. W. F. Bodtmann and C. L. Ruthroff, "Rain Attenuation on Short Radio Paths: Theory, Experiment, and Design," B.S.T.J., *53*, No. 7 (September 1974), pp. 1329–1349.
16. J. R. Norbury and W. J. K. White, "Point Rainfall Rate Measurements at Slogh, U.K.," Conference on Propagation of Radio Waves at Frequencies above 10 GHz, April 10–13, 1973, London, England, Conference Records, pp. 190–196 and IEE (London) Conference Publication Number 98.
17. B. J. Easterbrook and D. Turner, "Predication of Attenuation by Rainfall in the 10.7–11 GHz Communication Band," Proc IEE (London), *114*, No. 5, (May 1967), pp. 557–565.
18. K. Funakawa and J. Kato, "Experimental Studies of Propagational Characteristics of 8.6-m Wave on the 24-km Path," J. Radio Research Labs (Japan), *9*, No. 45 (September 1962), pp. 351–367.
19. K. Moritta and I. Higuti, "Statistical Studies on Electromagnetic Wave Attenuation Due to Rain," Review of the Electrical Communication Laboratories (Japan), *19*, No. 7–8 (July–August 1971), pp. 798–892.
20. A. L. Sims and D. M. A. Jones, "Climatology of Instantaneous Precipitation Rates," Illinois State Water Survey at the University of Illinois, Urbana, Illinois. Project No. 8624, March 1973.
21. C. L. Ruthroff, "Rain Attenuation and Radio Path Design," B.S.T.J., *49*, No. 1 (January 1970), pp. 121–135.
22. E. A. Mueller and A. L. Sims, "Investigation on the Quantitative Determination of Point and Areal Precipitation by Radar Echo Measurement," Technical Report ECOM-00032-F, Illinois State Water Survey at the University of Illinois, Urbana, Illinois, December 1966.
23. D. C. Hogg, "How the Rain Falls," unpublished work.
24. R. A. Semplak and R. H. Turrin, "Some Measurements of Attenuation by Rainfall at 18.5 GHz," B.S.T.J., *48*, No. 6 (July–August 1969), pp. 1767–1787 and Figure 11.
25. E. A. Mueller and A. L. Sims, "The Influence of Sampling Volume on Raindrop Size Spectra," Proc. Twelfth Conference on Radar Meterology, American Meteorological Society, October 1966, pp. 135–141.
26. J. O. Laws and D. A. Parsons, "The Relation of Rain Drop Size to Intensity," Trans. Am. Geophysical Union, *25*, 1943, pp. 452–460.
27. J. A. Morrison and M. J. Cross, "Scattering of a Plane Electromagnetic Wave by Axisymmetric Raindrops," B.S.T.J., *53*, No. 6 (July–August 1974), pp. 955–1020.
28. T. S. Chu, private communications.
29. T. S. Chu, "Rain Induced Cross Polarization at Centimeter and Millimeter Wavelength," B.S.T.J., *53*, No. 8 (October 1974), pp. 1557–1579.
30. W. T. Barnett, "Some Experimental Results on 18 GHz Propagation," The 1972 National Telecommunications Conference, December 4–6, 1972, IEEE, Houston, Texas, Conference Record, pp. 10E-1–10E-4 and IEEE Publication 72 CHO 601-5-NTC.
31. R. A. Semplak, "Effect of Oblate Raindrops on Attenuation at 30.9 GHz," Radio Science, *5*, No. 3 (March 1970), pp. 559–564.
32. Local Climatological Data, U. S. Department of Commerce, Environmental Science Services Administration, National Weather Records Center, Ashville, North Carolina, 28801. Also available from Superintendent of Documents, U. S. Government Printing Office, Washington, D. C. 20402.
33. J. Aitchison and J. A. C. Brown, *The Lognormal Distribution*, London: Cambridge University Press, 1957.

34. A. Papoulis, *Probability, Random Variables, and Stochastic Processes*, New York: McGraw-Hill, 1965, pp. 210 and 282.
35. P. Beckmann, *Probability in Communication Engineering*, New York: Harcourt, Brace and World, 1967, pp. 88 and 204.
36. G. H. Lentz and J. J. Kenny, private communication.
37. W. T. Barnett, H. J. Bergmann, and M. V. Pursley, private communication.
38. R. A. Semplak, "The Influence of Heavy Rainfall on Attenuation at 18.5 GHz and 30.9 GHz," IEEE Trans. Ant. Prop., *AP-18*, No. 4 (July 1970), pp. 507–511.
39. B. N. Harden, J. R. Norbury, and W. J. K. White, "Model of Intense Convective Rain Cells For Estimating Attenuation on Terrestrial Millimetric Radio Links," Elec. Letters, *10*, No. 23 (November 1974), pp. 483–484.
40. D. C. Hogg, "Intensity and Extent of Rain on Earth-Space Paths," Nature, *243*, June 8, 1973, pp. 337–338.
41. W. T. Barnett, "Multipath Propagation at 4, 6, and 11 GHz," B.S.T.J., *51*, No. 2 (February 1972), pp. 321–361.
42. R. R. Braham, Jr., and H. R. Byers, *The Thunderstorms*, Report of the Thunderstorm Project, Government Printing Office, Washington, D. C., 1949, Chapter VIII Squall Lines.
43. R. J. Boucher and R. Wexler, "The Motion and Predictability of Precipitation Lines," J. Meteorology, *18*, No. 2 (April 1961), pp. 160–171.
44. D. A. Gray, "Earth-Space Path Diversity Dependence on Base Line Orientation," 1973 International IEEE/G-AP Symposium and URSI Meeting, Boulder, Colorado, August 1973, Symposium Record pp. 366–369.
45. "Rainfall Intensity-Duration-Frequency Curves for Selected Stations in the United States, Alaska, Hawaiian Islands, and Puerto Rico," Weather Bureau, U. S. Department of Commerce, Tech. Paper 25, December 1955.
46. L. H. Seamon and G. S. Bartlett, "Climatological Extremes," Weatherwise, *9*, 1956, pp. 194–213.
47. A. E. Cole, R. J. Donaldson, R. Dyer, A. J. Kantor and R. A. Skrivanek, "Precipitation and Clouds, a Revision of Chapter 5, Handbook of Geophysics and Space Environments," AFCRL-69-0487, Air Force Surveys in Geophysics, No. 212, Office of Aerospace Research, U.S. Air Force Cambridge Research Laboratories, Bedford, Massachusetts, November 1969.
48. W. Y. S. Chen, private communication.
49. I. Anderson, "Measurements of 20 GHz Transmission Through a Wet Radome," 1973 International IEEE/G-AP Symposium and URSI Meeting, Boulder, Colorado, August 1973, Symposium Record, pp. 239–240.
50. A. J. Giger, "4-gc Transmission Degradation Due to Rain at Andover, Maine, Satellite Station," B.S.T.J., *44*, No. 7 (September 1965), pp. 1528–1533.
51. A. Cohen and A. Smolski, "The Effect of Rain on Satellite Communications Earth Terminal Rigid Radomes," Microwave J., *9*, No. 9 (September 1966), pp. 111–121.
52. D. Gibble, "Effects of Rain on Transmission Performance of a Satellite Communication System," IEEE International Convention Record, Part VI, March 1964, p. 52.
53. B. Blevis, "Losses Due to Rain on Radomes and Antenna Reflecting Surfaces," IEEE Trans. Ant. Prop., *AP-13*, No. 1 (January 1965), pp. 175–176.
54. B. Blevis, "Rain Effects on Radomes and Antenna Reflectors," Proc. IEE Conference on Large Steerable Aerials, London, 1966, pp. 148–152.
55. H. J. Bergmann and S. H. Lin, "Measurements of 12 GHz Transmission Loss Through a Wet Radome," unpublished work.